Dynamic Characteristics of Timber Bridges as a Measure of Structural Integrity

Angus Morison[1], C.D. VanKarsen[1], H.A. Evensen[1], J.B. Ligon[1], J.R. Erickson[3], R.J. Ross[2], and J.W. Forsman[3]

[1]Dynamic Systems Laboratory
Michigan Technological University
1400 Townsend Drive
Houghton, MI 49931

[2]Forest Products Laboratory
USDA Forest Service
One Gifford Pinchot Drive
Madison, WI 53705-2398

[3]School of Forestry & Wood Products
Michigan Technological University
1400 Townsend Drive
Houghton. MI 49931

ABSTRACT

Bridges require periodic inspections to ensure the safety of those using the structure. A myriad of techniques have been developed in order to quickly and accurately determine a structure's health. Unfortunately, timber structures are still, in most cases, subjectively evaluated. Decay is one of the most common damage mechanisms in these structures, and often inflicts damage internally, without visible signs appearing on the surface until a timber's load bearing capacity has been largely destroyed. Steel and concrete structures have been successfully evaluated with a variety of dynamic nondestructive methods, using a structure's modal properties to detect and locate damage. This paper presents an extension of several previously developed dynamic nondestructive methods to timber bridge structures.

NOMENCLATURE

FRF	frequency Response Function
mDOF	measured degree of freedom
$[\Phi]$	mass normalized mode shape matrix
$[H(jw)]$	frequency response function matrix
M_{Af}	Modal A for the r^{th} mode
Ψ_{pr}	response of point p for r^{th} mode
λr	r^{th} eigenvalue of system
y_i	displacement of point *i*
h	spacing between each DOF
C	measured curvature
C′	calculated curvature
δ	damage index
[F]	flexibility matrix
BGCI	bridge girder condition index
Δ	deflection calculated by flexibility method
*	used to denote complex conjugate

1. INTRODUCTION

Engineered structures require rigorous and timely inspections to ensure structural performance. In general, damage detection requires that some indicating parameter be monitored that is sensitive to the damage mechanism in question. Many inspection techniques are available for civil engineering structures, with varying levels of information provided by each method. The goal of this research is to investigate several existing methods that have shown promise on other types of structures, and apply them to short span timber bridge structures. The impetus for this work is a desire to employ a quantitative, global inspection method on these structures. Currently employed quantitative methods, such as stress wave timing, provide damage information for a very localized area only. Also, the most common bridge inspection technique - visual inspection - is highly subjective and overly reliant on the inspector's experience and judgment.

Short span timber bridges are the focus of this paper. These bridges are found extensively throughout our national forests. As well as recreational traffic, these bridges are subject to extremely high loads from logging companies moving capital equipment as well as cut logs in and out of the national forests. Figure 1 shows photographs of a typical bridge. Most of the bridges germane to this study are comprised of a single span with an average overall length of about 20 feet. Ten stringers with an average size of 6 inches wide by 16 inches deep comprise the substructure of the bridge. The stringers are covered by 3 inch high by 8-inch wide deck boards nailed perpendicular to the stringers. Finally, to provide a durable surface for traffic, 3 inch tall by 10 inch wide planks are nailed in two strips parallel to the direction of the stringers to create the driving surface.

A literature review was completed to identify existing damage detection schemes that could be especially useful in the context of timber bridges. Two methods were selected and investigated. The first method described uses estimates

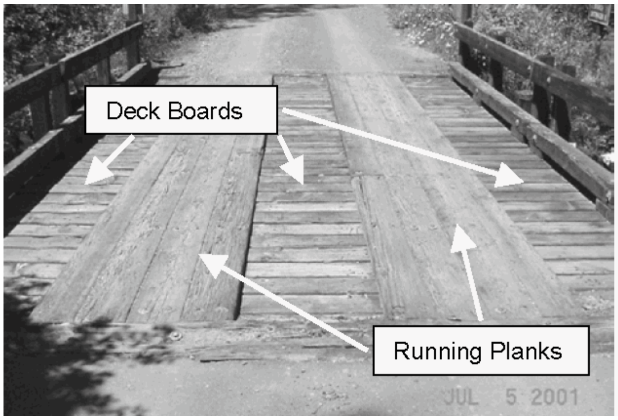

a) Top View of Bridge Deck

b) Side View of Bridge Deck

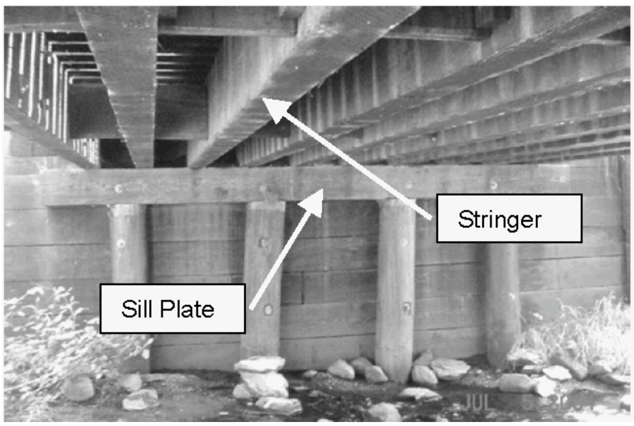

c) View of Bridge Deck Underside

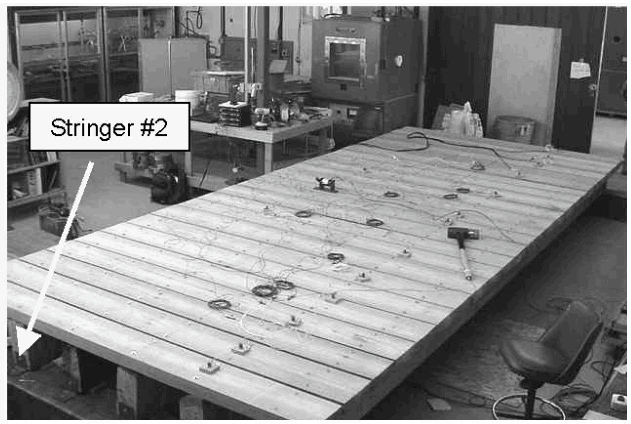

d) Laboratory Bridge at MTU

Figure 1 - Structural Details of a Typical Bridge Under Test (a, b, c) and Laboratory Bridge (d)

of the surface strain or curvature of the structure to identify damaged areas. The particular implementation of curvature data is highly useful for this problem because it requires no baseline model, and attempts to locate damage solely from the structure's response at time of test. Baseline models are generally not available for these bridges, which are in various states of decay and are typically 40-50 years old. The second method uses flexibility influence coefficients to estimate the static deflection properties of the structure from modal data. This method was shown to be very effective in locating damage in steel stringer, concrete deck bridges. Its past success with bridges of similar design makes this method an obvious choice for investigation.

These methods were investigated in a laboratory setting designed to simulate short span timber bridges found throughout our national forests. A bridge was constructed in the lab at Michigan Technological University using a design similar to the field bridges. The laboratory bridge is shown without rails in Figure 1.d. although it was tested with a rail system attached. Six 6 inch by 12 inch stringers, spaced 18 inches on center, were used to create a span of 20 feet, simply supported on both ends. A deck of 3 inch by 8 inch boards was attached perpendicular to the stringers and a rail system was also added. Damage was simulated in the structure by replacing 1 of the original stringers used in the bridge's construction (stringer #2) with a stringer whose El Product was 33% (see Table 1) less than the original. Figure 2 shows the layout of measurement points used throughout this paper on the laboratory bridge's deck. Each row of measurement points was located on the deck directly above a stringer, spaced 18 inches apart. creating an 18x18 inch grid on the bridge surface. Stringer #2 fell underneath mDOFs 16-30.

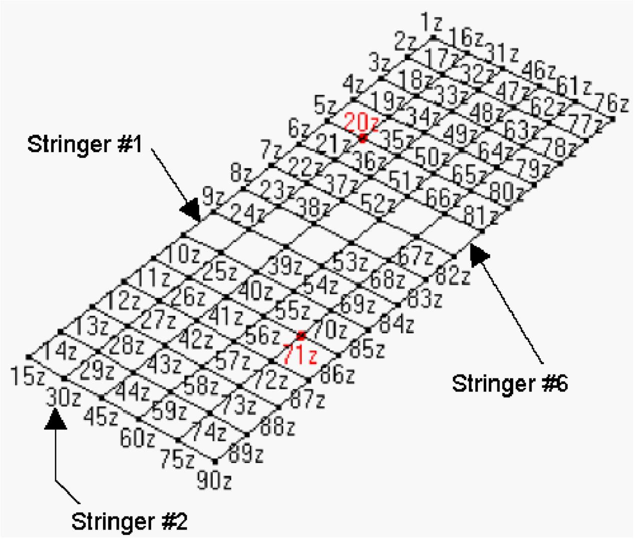

Figure 2 - Layout of mDOFs on Laboratory Bridge Deck

	Stringer (all approx. 6" wide by 12" tall)					
	#1	#2	#3	#4	#5	#6
Original Configuration	1.19	0.88	0.78	0.61	0.92	1.17
Stringer #2 Replaced	same	0.58	same	same	same	same

Table 1 - Elastic Modulus of Stringers Used in Lab Bridge Construction (Mpsi)

2. MODAL CURVATURE

2.1 Theory and Background

Mode shapes have been widely investigated as a damage indicator for several reasons. First, they contain information about every measured degree of freedom (mDOF) on the structure. Since they are also very closely related to the mass and stiffness matrices of a particular structure, changes to the structure should be observable in the mode shape vectors. Furthermore, it is often theorized that spatially discrete discontinuities in mode shapes correspond to possible damaged areas. Mode shape data can be viewed in many forms. Most commonly, a translational measure such as acceleration, velocity, or displacement is used to visualize the mode shape vectors. An alternative is to record (with strain gages) or process (from translational measurements) the data into curvature mode shapes. Here the values of the mode shape vector residues are a measure of the local surface curvature of the structure. The method investigated here utilizes this perspective. Furthermore, Ratcliffe et al [1] has extended the analysis from modal curvature vectors to FRFs themselves. The benefits of this are easy to see. The time to process a set of FRFs into a valid and representative set of mode shapes can be quite lengthy, and generally requires a data analysis software program. Also, the user of the test must possess advanced training required to perform modal analysis. By eliminating these requirements, the damage detection process can be automated. Another benefit of this analysis is that a pre-existing baseline model is not needed, which, as discussed earlier, is strongly desirable for these in-place structures. A much more in-depth discussion of the benefits and development of this method is presented by Ratcliffe et al in references [1] and [2].

2.2 Experimental Data and Processing

The experimental data used in this analysis is a set of inertance FRFs. Fifteen evenly spaced mDOFs were deployed along the length of each stringer (see Figure 2), for a total of 90 FRFs. To implement the method, inertance measurements were converted to curvature measurements at each frequency, for each stringer. This provides six sets of damage indices for each bridge configuration. It is hypothesized that changes to any of the stringers will be visible in the stringer's curvature damage index plot. Since the measurements are complex inertance measurements, this was done separately for the real and imaginary parts of the measurement, generating real and imaginary curvature estimates. Although many estimation techniques are available, equation (1) shows the finite difference approximation used.

$$C_i = (y_{i+1} + y_{i-1} - 2y_i)/h^2 \qquad (1)$$

The calculated curvatures represent the true behavior of the structure. A damage index must now be formed by comparing the behavior of the structure as tested to some sort of predicted or baseline behavior. The baseline curvature of the structure at each mDOF is estimated from the measured data using what is described as a gapped polynomial [1], making use of the measured curvatures from adjacent mDOFs along each stringer. Specifically, four other measured curvatures are used. When possible, two mDOFs from each side are employed. This is not possible for the first and last two points along each stringer, which are estimated from the four points directly following or preceding the point. The second and second-to-last points use the first or last points respectively, as well as the three following or preceding points. These measurements are used to calculate the coefficients of a third order polynomial (see equation (2)), and from these coefficients, the curvature of the point in question can be estimated (equation (3)). The damage index is simply the difference squared between the estimated and measured curvature at each point, for every frequency, as seen in equation (4). Since the data is complex, the differences in the real and imaginary portions are squared and combined to form a single damage index. The final step is to normalize the results. In this work, the data was normalbed by setting the mean damage index at each frequency line, for each stringer, equal to unity.

$$\begin{Bmatrix} C_{i-2} \\ C_{i-1} \\ C_{i+1} \\ C_{i+2} \end{Bmatrix} = \begin{bmatrix} 1 & x_{i-2} & x_{i-2}^2 & x_{i-2}^3 \\ 1 & x_{i-1} & x_{i-1}^2 & x_{i-1}^3 \\ 1 & x_{i+1} & x_{i+1}^2 & x_{i+1}^3 \\ 1 & x_{i+2} & x_{i+2}^2 & x_{i+2}^3 \end{bmatrix} \begin{Bmatrix} p_{0_i} \\ p_{1_i} \\ p_{2_i} \\ p_{3_i} \end{Bmatrix} \tag{2}$$

$$C_i' = p_{0_i} + p_{1_i} \cdot x_i + p_{2_i} \cdot x_i^2 + p_{3_i} \cdot x_i^3 \tag{3}$$

$$\delta_i = (C_i' - C_i)^2 \tag{4}$$

2.3 Results

Since this method provides information at each spectral line, as well as for each mDOF, the results are best displayed as a colormap, with an independent axis for spectral lines, an independent axis for mDOF, and damage index corresponding to color. Figure 3 shows the results for the first and second stringer, before and after the second stringer was replaced. This broadband display of results helps eliminate one of the drawbacks associated with the use of mode shapes: that mode shaped based damage indications are extremely sensitive to the modes used. Credence to this statement can be seen in the damage index plots for stringer #1. At particular mDOFs, the damage index only becomes high in certain frequency ranges, ie, for

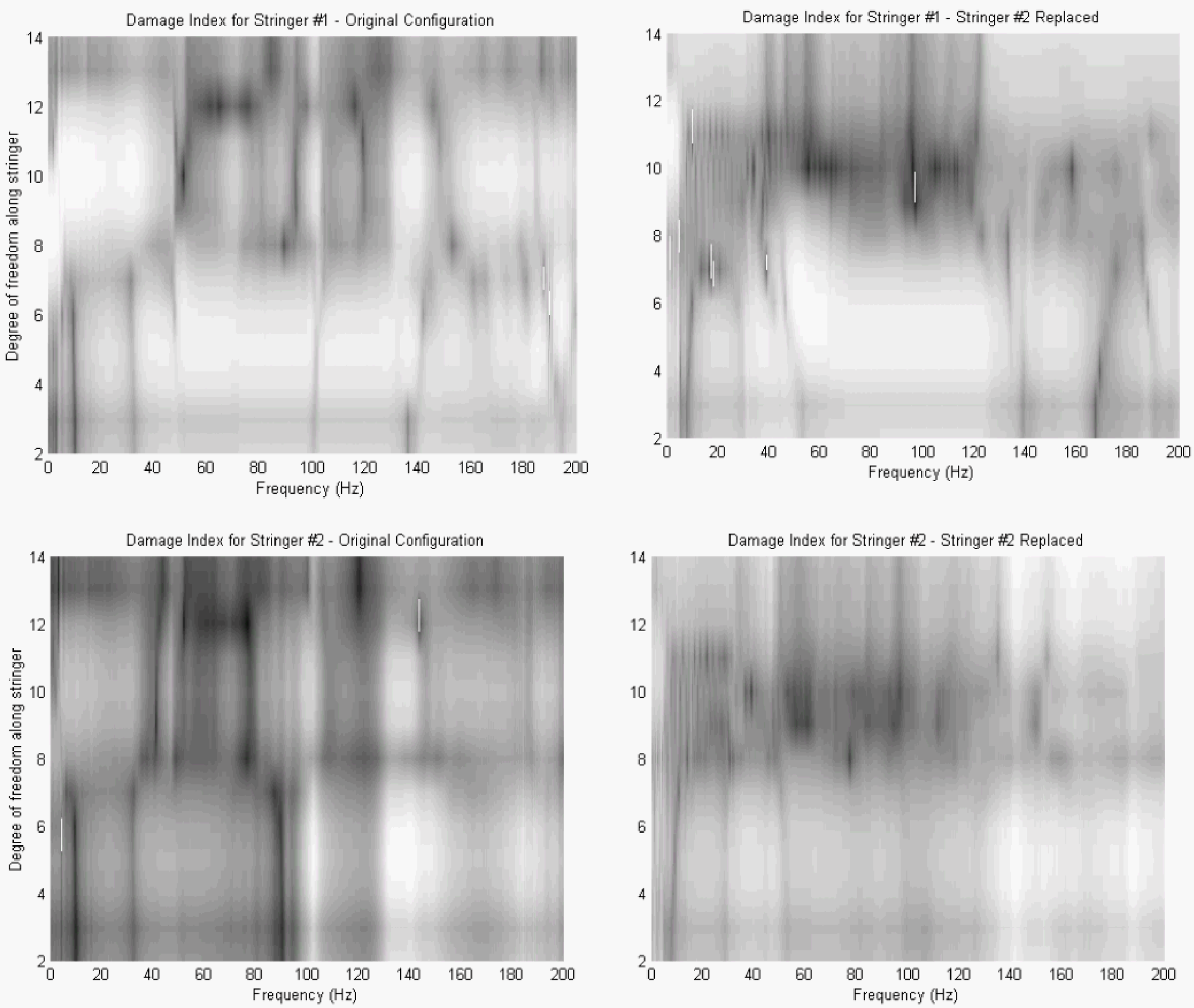

Figure 3 – Curvature Based Damage Index
(Lighter shade means higher damage index value)

certain modes of vibration. The broadband formulation allows any mDOF for which a significant frequency range shows a high damage index to be investigated as a possible damage site.

Detecting changes to the structure with this method is difficult however. By inspection of the stringer #2 damage indices, significant differences can be seen. Differences, although less pronounced, also appear in the stringer #1 results. It is clear that the structure has been changed but it is unclear exactly what type of change has occurred. Ambiguity in the results can be partially attributed to the curvature method itself. The method is more applicable in cases where the damage occurs in a very localized area. In the case where the entire stringer's mechanical properties have degraded, measurements along each stringer should still result in a fairly continuous curvature function, without the type of discontinuities that are easy to detect with gapped polynomial estimation.

3. FLEXIBILITY INFLUENCE COEFFICIENTS

3.1 Theory and Background

Flexibility influence coefficients can be defined in a number of ways. In non-mathematical terms, the flexibility coefficient between two DOFs can be described as the deflection at a particular DOF due to a unit load at another DOF. If all of the influence coefficients are known, any type of static loading pattern on the structure can therefore be simulated. Mathematically, the most basic definition of flexibility is that the matrix of flexibility influence coefficients is the inverse of the stiffness matrix of a particular system [3]. Since the stiffness matrix is generally not available for most systems of interest, this definition is usually not particularly useful. The flexibility coefficients, however, can also be derived from modal data. Historically the flexibility matrix can be defined using the unity modal mass scaled mode shape vector and the diagonal natural frequency matrix, as seen in equation (5) [7]. Scaled mode shapes are not always readily available however, especially in the case of ambient excitation modal analysis, which is common on large bridge structure. An even more convenient estimate of the flexibility matrix is available which neutralizes this shortcoming. Catbas et al [4,5,6] have shown that the flexibility matrix can be estimated by the DC value of the FRF matrix. Equation (6) shows this relation. It is this method of developing the flexibility coefficients that is utilized in this paper.

$$[F] = [\Phi][\Omega]^{-1}[\Phi]^{T} \qquad (5)$$

$$F_{ij} = H_{ij}(j\omega = 0) = \sum_{r=1}^{N} \left[\frac{\psi_{ir}\psi_{jr}}{M_{A_r}(-\lambda_r)} + \frac{\psi_{ir}^{*}\psi_{jr}^{*}}{M_{A_r}^{*}(-\lambda_r^{*})} \right] \qquad (6)$$

Flexibility coefficients as a damage index have been successfully used for locating simulated damage in a steel stringer, concrete deck, highway bridge [4,5,6]. This success dictates that flexibility coefficients are a strong candidate for the timber bridge problem. Unlike the curvature method, however. this analysis requires some sort of baseline model for comparison, whether it be a finite element model, or the initial test data for a structure.

3.2 Experimental Data and Processing

Multi-reference impact testing, using points 20 and 71 as driving points (see Figure 2). was performed on the original and modified laboratory bridge. Commercially available software packages were used to estimate the modes of vibration of the structures in the range of 0 to 100 Hz. Table 1 summarizes the modal results. Modes appearing in the same row of the table are correlated with a modal assurance criterion of greater than 0.75. The modes described in Table 2 were used to synthesize the entire FRF matrix and subsequently create the flexibility matrix.

The measured inertance FRFs of a structure were used to estimate the flexibility coefficient matrix for the structure using equation 6. An error, however, can be introduced into the flexibility calculation due to modal truncation. The flexibility estimate is tied to the number of modes used to synthesize the FRF. Every mode above the frequency range curve-fitted adds to the true value of flexibility, but is not accounted for in the estimate, leading to error. In practice, a critical number of modes can be identified such that adding more modes to the FRF synthesis does not significantly change the flexibility estimate.

Modal Frequencies (Hz)	Original Configuration	Stringer #2 Replaced
	9.12	8.75
	9.79	9.77
	32.19	29.69
	32.44	32.31
	47.06	43.87
		46.44
	50.81	52.26
	53.87	
		62.46
		66.06
	67.56	70.56
	87.31	84.69
	96.69	94.81

Table 2 - Modal Comparison

In order to lend greater physical significance to the flexibility coefficients, a deflection pattern due to a physically significant load pattern can be investigated. Catbas et al [4,5,6] proposed a measure which looks at each stringer separately, called the bridge girder condition index (BGCI), since the primary area of concern is damage to the stringers. To include information available in the off diagonal terms of the flexibility matrix, and not just the major diagonal, a unit load pattern is applied to each of the stringers. The result is an estimate of the deflection due to a line load running the length of the stringer. Equation (7) explains the calculation

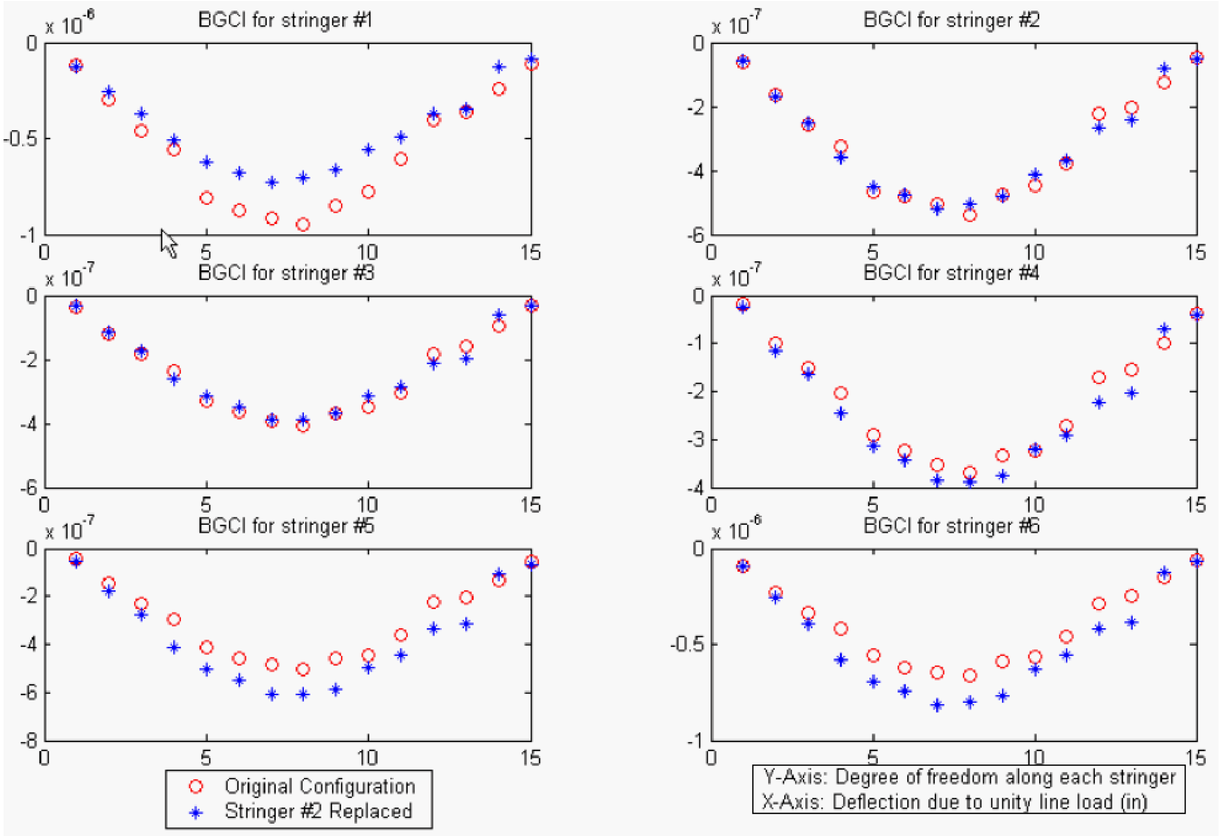

Figure 4 - Simulated Deflections from a unity-valued line bad placed directly above each stringer

of the BGCI. Each submatrix in equation (7) represents a 15 element (one element for each DOF on the stringer) column matrix, with one submatrix for each stringer. The BGCI was calculated for each stringer in each configuration of the bridge. Equation (7) shows an example for calculating the BGCI of the third stringer.

$$BGCI_3 = \begin{Bmatrix} \{0\} \\ \{0\} \\ \{\Delta_3\} \\ \{0\} \\ \{0\} \\ \{0\} \end{Bmatrix} = [F]_{90x90} \begin{Bmatrix} \{0\} \\ \{0\} \\ \{1\} \\ \{0\} \\ \{0\} \\ \{0\} \end{Bmatrix} \qquad (7)$$

3.3 Results

The initial bridge configuration was used as a baseline for comparison to the bridge built with the weaker stringer. Figure 4 shows the results for each of the six stringers. The expected result is that the BGCI for the stringers after the configuration change should have shown more displacement, especially for stringer #2. This hypothesis proved only partially true. The BGCI for stringers #4 to #6 showed increased deflection but stringers #2 and #3 showed almost no change. Stringer #1 had less predicted deflection. This data would lead one to conclude that the bridge sustained some damage, especially in stringers #4 to #6. Of course, this doesn't help predict that change that was actually made to the structure, damage to stringer #2.

4. CONCLUSIONS

This paper presented several damage detection schemes for possible implementation with timber bridge systems. Pure inspection of the modal data showed slight changes in frequency and mode shape for most modes, but it was unclear how the changes related to the structure's properties. The broadband curvature method was also successful in showing a difference from the original state to the damaged state. Furthermore, changes to the damage index appeared more pronounced for stringer #2 than for other stringers. This, however, is far from a quantitative prediction of damage. Finally, the flexibility coefficients method was definitely able to show a difference in the bridge with the replacement of stringer #2. Taken on the whole, since five of six estimates showed increased deflection or no change, one could draw the conclusion that the overall bridge system has a lower EI product [8]. This in fact is a true statement. The method, however, failed to identify that stringer #2 was changed, leaving all others alone.

5. ACKNOWLEDGEMENTS

The authors wish to thank the U.S. Federal Highway Administration and the U.S. Forest Service for funding this work. Within the Forest Service, the authors would specifically like to recognize the people of the Ottawa National Forest and the Chequamegon National Forest for locating and directing us to bridges suitable for this study. Finally, the authors would like to thank PCB Piezotronics for its help in providing much of the equipment used in this work.

6. REFERENCES

[1] **Ratcliffe, C.P., Bagaria, W.J.** *A Vibration Technique for Locating Delamination in a Composite Beam.* AIAA J., 36, No. 6, pp. 1074-1077.

[2] **Ratcliffe, Colin P.** *A Frequency and Curvature Based Experimental Method for Locating Damage in Structures.* Journal of Vibration and Acoustics, V. 122, No. 3, pp. 324-329.

[3] **Rao, Singiresu S.** *Mechanical Vibrations, 3rd Edition* Addison Wesely Publishing Company, Reading, Mass, 1995

[4] **Catbas, F.N., Lenett, M., Brown, D.L., Doebling, S.W., Farrar, C.R., Turer, A.** *Modal Analysis of Multi-Reference Impact Test Data for Steel Stringer Bridges.* Proceedings of the 15th International Modal Analysis Conference, 1997.

[5] **Catbas, F.N., Lenett, M., Aktan, A. E., Brown, D.L., Helmicki, A.J, Hunt, V.** Damage Detection and Condition Assessment of Seymour Bridge. Proceedings of the 16th International Modal Analysis Conference, 1998.

[6] **Aktan, E., Brown, D., Farrar, C., Helmicki, A., Hunt, V., Yao, J.** Objective Global Condition Assessment. Proceedings of the 15th International Modal Analysis Conference, 1997.

[7] **Doebling, Scott W., Farrar, Charles R.** *Computation of Structural Flexability for Bridge Health Monitoring Using Ambient Modal Data.* Proceedings of the 11 h ASCE Engineering Mechanics Conference, 1996

[8] **Ross, R.J., Hunt, M.O., Wang, X., Soltis, L.A.** *Floor Vibration: A Possible Assessment Method for Historic Buildings.* APT-Bulletin –TheJournal of Preservation Technology: 32(2-3): 23-25. 2001.

Proceedings, IMAC-XXI, a conference on
structural dynamics, 2003 February 3-6, Kissimme, FL.
(Published on CD-ROM.)